

# Low-level Laser Therapy Device for Assisting Distraction Osteogenesis in Maxillofacial Reconstruction Applications

Toktam Jafarpour<sup>1</sup>, Farouk Smith<sup>2\*</sup>

1. Department of Mechatronics Engineering, Nelson Mandela University, Port Elizabeth, South Africa,  
Email: s223513377@mandela.ac.za

2. Department of Mechatronics Engineering, Nelson Mandela University, Port Elizabeth, South Africa.  
Email: farouk.smith@mandela.ac.za (Corresponding Author)

Received: 3 November 2022    Revised: 15 December 2022    Accepted: 6 January 2023

## ABSTRACT:

In different medical applications, physical stimulation techniques are used to assist the treatment and improve the treatment conditions from different perspectives. They can accelerate the healing process and stimulate biological processes and healing mechanisms. In oral and maxillofacial reconstruction, one of the widely used physical stimulation techniques is Low-Level Laser Therapy (LLLTT). LLLTT is a photonic stimulation technique that accelerates the biological processes of the cells and healing mechanisms. In LLLTT, light photons are used to physically impact the healing zone. Distraction Osteogenesis (DO) is a novel reconstruction technique that is used for tissue regeneration in different body zones. By using DO, acquired and congenital bone defects can be reconstructed. Recent experimental studies show that in a DO treatment, the application of LLLTT during bone regeneration process can significantly improve the outcome of the treatment and enhance the quality of the regenerated bone tissue. In this research a LLLTT device is proposed to be used during DO in maxillofacial reconstruction applications. The results of this study show that the proposed device can generate single- and multi-wavelength laser lights with controlled parameters. The proposed system can be used during the DO treatment to shorten the treatment time and improve the quality of the outcome and treatment conditions.

**KEYWORDS:** Maxillofacial Reconstruction, Photonic Stimulation, Medical Device, Physical simulation; Distraction Osteogenesis.

## 1. INTRODUCTION

In Maxillofacial Reconstruction Applications (MRA), different surgical methods have been used for the reconstruction of different defects, including Distraction Osteogenesis (DO), bone grafting, prosthetics, and vascularized flap. Among the mentioned reconstruction techniques, DO is a novel limb lengthening method for the reconstruction of skeletal defects and deformities. This technique is known as a solution without the need for a bone graft. The application of DO technique has recently been emerging in MRA [1-4]. In a DO process in MRA, the defected bone is osteotomized and a distractor is fixed to the bone part. The distractor could be either a manual or an automatic distractor. The distractor can apply a distraction force to the bone part and moves it in a linear vector toward the destination point. During this process, new bone tissue is generated and fills the gap between the bone part and the main bone segment. Thus, generated gap is filled with newly formed bone tissue [5-7]. By using this technique, the treatment time

is reduced and the quality of the reconstructed tissue is improved. Also, a more stable treatment process, as well as a predicted outcome, could be achieved. By using the DO technique, the side effects of the reconstruction process, as well as patient discomfort, is reduced. The DO can also reduce scar formation and pain compared to other reconstruction techniques [8], [9].

Different Physical Stimulation Techniques (PSTs) have been developed to assist the DO process and to improve the outcome of the DO treatment [10]. Fig. 1 illustrates the role of DO treatment and the application of PSTs in MRA. PSTs can be divided into four categories, namely the photonic, electromagnetic, electrical, and mechanical techniques. The photonic stimulation techniques can affect the healing mechanisms using light photons. In electromagnetic techniques, the presence of the magnetic field can affect the healing mechanisms. The electrical stimulation techniques can affect the healing process using electrons, and the mechanical stimulation

techniques can influence the healing process by using energy packets by mechanical means [11], [12].

Photonic stimulations are a category of advanced techniques that use specific wavelengths to create therapeutic effects. In the reconstruction of the oral and maxillofacial area, Low-Level Laser Therapy (LLLT) has been widely used. In a LLLT method, low-power laser light is used to emit photons toward the healing zone. LLLT can influence the healing process by positively inducing the function and the activity of the mitochondria, consequently, the cell synthesizes a larger amount of adenosine triphosphate, which causes

it to produce more energy. The more energy, the better the function of the cells and the healing process [13], [14]. The application of LLLT during tissue healing results in the enhanced efficiency of the cells. The cells can rejuvenate themselves better and repair the damage [15]. In the reconstruction of the oral and maxillofacial area, LLLT can decrease pain and reduce bone swelling during the process. The LLLT has been used during different medical procedures including DO, bone graft, wound healing, bovine bone graft, pre-implant tissue healing, and autogenous [16-24].

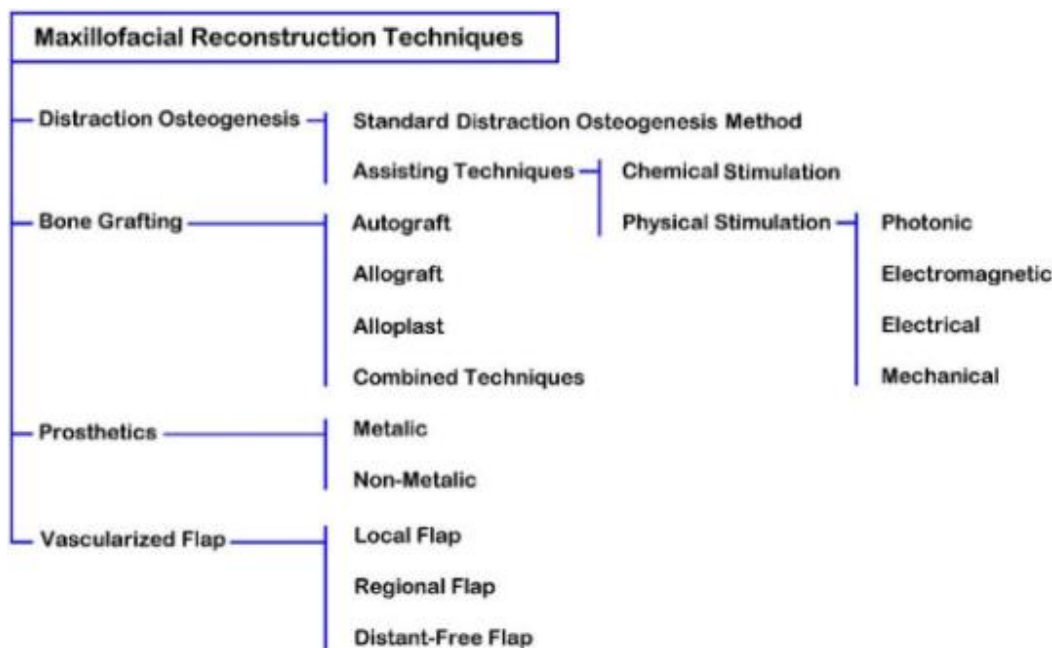


Fig. 1. The role of DO treatment and the application of PSTs in MRA [11]

### 1.1. LLLT for Assisting DO

LLLT is an assistive technique that has shown superior results in assisting DO treatment. In the LLLT, different types of laser emitters can be used as a light source. Studies have shown that these effects are dependent on the wavelength of the laser light as well as the output power of the laser light that is delivered to the tissue. During a DO treatment, LLLT can enhance bone formation mechanisms, accelerate the metabolic functions of the cells during bone healing, and relieve pain [25], [26].

In the last two decade, the application of LLLT during DO has been under investigation. In a study performed in 2007 [27], the effects of applying LLLT during the DO treatment on a sheep model were investigated. In this study, a single-wavelength laser light, Ga-Al-As laser, with a treatment dose of 4 J/cm<sup>2</sup>, and a total dose of 16 J/session, was used. In this study, the intermittent emission mode for generating and emitting the laser light, with an activation sequence of

5 times daily, was used. In another study in 2007, on a rabbit model [14], the same laser light, Ga-Al-As laser, with a treatment dose of 6 J/cm<sup>2</sup>, and a total dose of 36 J/session, was used. The laser light was emitted onto the distraction zone one time daily. In an experimental study in 2012 [28], a sheep model was used to evaluate the effects of applying a higher dose of Ga-Al-As laser light compared to previous studies. In this experimental study, the laser light was emitted onto the distraction zone at four predetermined points, with a total delivered energy of 120 J/cm<sup>2</sup>. Also, in this study, a continuous emission of the laser light was used.

In 2015, in a clinical trial on humans [29], a Ga-As laser with a wavelength of 905 nm was used. The laser light was intermittently emitted onto the distraction zone, at four pre-determined zones with a dose of 5 16 J/cm<sup>2</sup>, and a total delivered energy of 20 J/session. In this trial, the LLLT was used for 12 sessions in 24 days, 2 min/session. In 2016, LLLT was used during the DO on a rabbit model [30]. In this research work,

an 830 nm laser with intermittent emission, at 4 pre-determined zones was used. The LLLT was used with a dose of  $5 \text{ J/cm}^2$  and a total delivered energy of 200 J/session. In a recent animal study in 2018 [31], a dog model underwent DO for the reconstruction of the mandible. During this animal study, LLLT was assisting the DO. In this study, a laser with a wavelength of 970 nm and output power of 2W, with an intermittent emission of LLLT, was used, while the laser light was emitted onto the distraction zone with a total delivered energy of 840 J/session. During the consolidation phase, the LLLT was used in continuous emission for two minutes, five times daily.

In a recent study in 2021 [32], the application of diode lasers in assisting the DO technique during MRA was studied. In this experimental study, a rabbit model was used. The rabbits underwent mandibular distraction osteogenesis while the diode laser was emitted onto the distraction zone to positively affect the reconstruction process and bone cell regeneration. During the consolidation phase of the treatment, the test group was treated with laser light, with a dose of  $10 \text{ J/cm}^2$ , every 28 hours, for a treatment period of one to four weeks (3 to 12 laser therapy sessions). The results of performed experimental studies as well as clinical trials have revealed that the LLLT has a direct effect on the mitochondria of the cells in the injured/healing tissue [33]. The LLLT technique has stimulating, healing, and restoring effects and can positively affect the quality of the outcome of the DO treatment.

It can be seen in the performed studies that there are different conditions in which the LLLT can assist the DO process. It depends on the condition of the DO treatment, the nature of the defect, the method of reconstruction, and the LLLT method that is used in that specific treatment. Therefore, the LLLT device should have the capability of working in various conditions. The output energy, the wavelength of the laser light, the working conditions, and single/multi-wavelength methods are the factors that need to be set

when the LLLT system is assisting the DO process. In this research, a multi-wavelength LLLT device for assisting DO in MRA is proposed. The developed method can perform LLLT in single- and multi-wavelength modes. By using the proposed device, a LLLT technique, with controllable intensity of the generated and emitted laser lights and activation intervals, can be enabled. The proposed system can run a fully automatic LLLT during DO treatment with controlled laser emission.

## 2. MATERIAL AND METHODS

### 2.1 Design of the LLLT Device

To design a multi-wavelength LLLT device for assisting the DO method, different electronic components and mechanical parts should be used. Fig. 2 illustrates the block diagram of the designed system. For generating low-power laser light with controlled output power, in multi- and single-wavelength modes, different units need to be used within the designed system. Fig. 2 illustrates the overall design of the proposed multi-wavelength LLLT device. In this system, a microcontroller is used as the control unit of the device. A power supply is used in the design of the system for providing the required power for the device. Two laser beams with specific wavelengths are used in the design of the system for generating the low-level laser. A laser beam driver is used within the design of the system for activating and deactivating the laser modules. By using these laser beam drivers, adjusting the output power of the device is possible. In addition, a linear stepper motor is used in the system for focusing the generated laser light. The implemented microcontroller can automatically control the generation of the low-level laser light using the set data. A human-machine interface, including a liquid crystal display (LCD) and a keypad, is connected to the control unit of the system for setting the working parameters of the device.

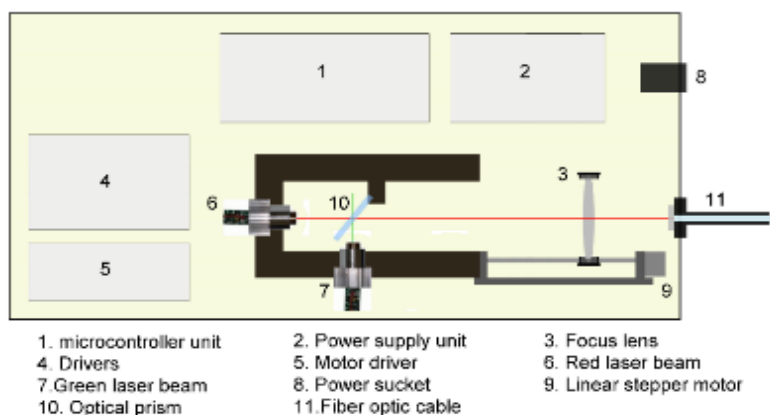


Fig. 2. The overall design of the proposed multi-wavelength LLLT device.

A power supply, S-60-12 12V 5A DC power supply, is used in the design of the system. The power supply is connected to the implemented microcontroller, laser beam driver, and stepper motor driver. In the control system, an ARDUINO MICRO A000053 development MCU board is used as the controller. In the ARDUINO MICRO development board, an ATMEGA32U4 controller is used. The ATMEGA32U4 provides 20 digital input/output ports. Among 20 digital pins, 7 pins are PWM pins. In this development board, a crystal with a clock frequency of 16 MHz is used. The digital input/output pins of the microcontroller are connected to the laser beam driver and the stepper motor driver. Also, in the designed system, a MX1508 dual H-channel driver, designed with N-channel and P-channel power MOSFETs, with a maximum drive current of 2 A and maximum operation voltage of 10 VDC, is used. By implementing these connections between the control unit and the laser beams driver, controlling the activation of each laser beam as well as their intensity is possible.

For driving the linear stepper motor, a L298N dual full-bridge driver, with maximum drive current of 2 A and maximum operation voltage of 46 VDC, is used. Two digital PWM pins are connected to the laser beams driver for driving the laser module and adjusting the intensity of the output power using PWM signals. By implementing these connections between the control unit and the laser beam drivers, controlling the

activation of each laser beam as well as their intensity is possible. For controlling the performance of the stepper motor, 4 digital pins of the microcontroller are used and connected to the motor driver. By using these 4 pins, the control unit can control the performance of the linear stepper motor.

In the designed system, a linear stepper motor, D8-MOTOR80 two-phase mini linear stepper motor, with a stride angle of  $18^\circ$  is used. The output pins of the L298N motor driver are connected to the inputs of the D8-MOTOR80 two-phase mini linear stepper motor. These connections can activate the stepper motor's coils with predetermined sequences. Therefore, the linear position of the carriage of the stepper motor can be controlled and set. A focusable Biconvex lens is implemented within the system for focusing the generated laser light. The moving focus lens is fixed to the carriage of the mini linear stepper motor. Therefore, controlling the linear positioning of the lens and focusing the laser light is possible. In addition, a human-machine interface (HMI) unit is used to enable the setting and modification of the working parameters of the system. The HMI unit consists of a 4-key membrane keypad and a character LCD. A limit switch is used within the design of the system to limit the stepper motor's movement and to determine the start position of the stepper motor's carriage. Fig. 3 illustrates the overall design of the control system of the proposed multi-wavelength LLLT device.

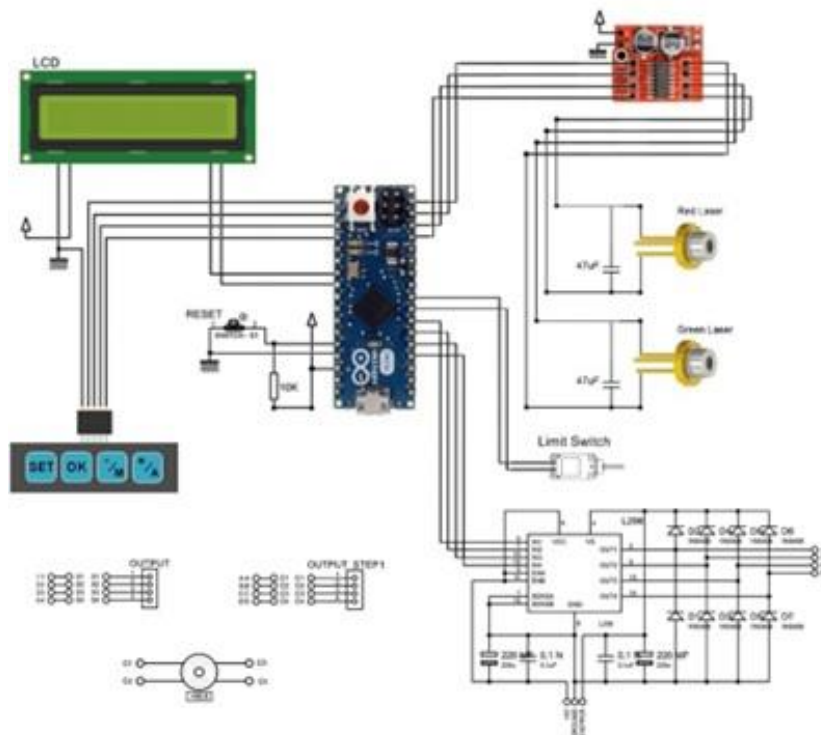


Fig. 3. The overall design of the control system.

In the design of the system, two laser beams with specific wavelengths, including a red laser beam with a wavelength of 650 nm and output power of 50 mW, and a green laser beam with a wavelength of 532 nm and output power of 50 mW, are used. Fig. 4 illustrates the implemented laser beams in the developed prototype of the LLLT system. When the system is run, the laser lights are generated using predetermined working factors. The generated laser lights are reflected onto the optical prism. The optical prism can align these two laser lights. In addition, there is a focus lens

in front of the optical prism for focusing the transmitted light onto the entrance of an optical fiber. The linear stepper motor can precisely set the position of the focus lens. Therefore, the positioning of the stepper motor's carriage during the movement can be calculated, based on the open-loop control system parameters. By controlling the linear position of the carriage of the linear stepper motor, controlling the position of the focus lens is possible. Afterwards, the low-level laser light can be transferred to the distraction zone using the fiber optic cable.

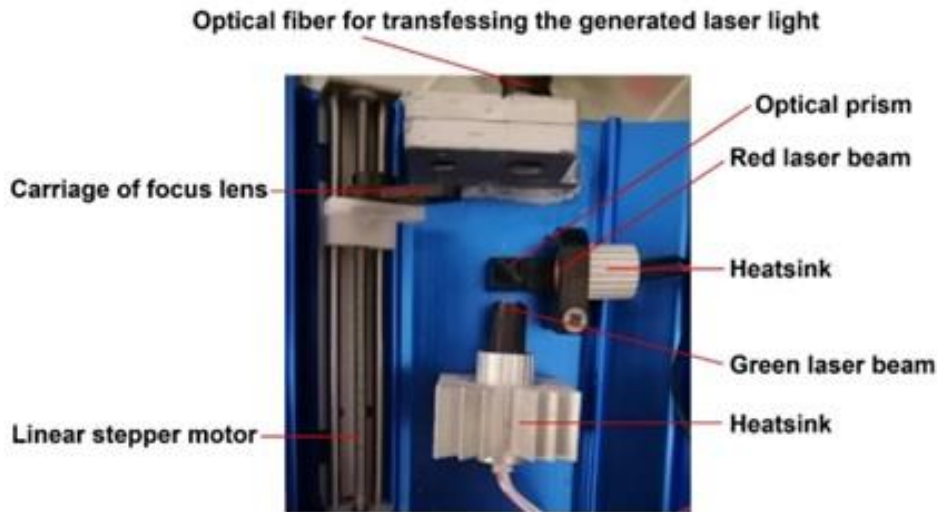


Fig. 4. The implemented red and green laser beams in the LLLT system.

2.2 Modeling of the Control System

The designed control system has been simulated and modeled using MATLAB/SIMULINK software. The designed controller is capable of driving the linear stepper motor that is implemented within the designed system. The designed control system is capable of controlling the stepper motor in different working states with various angular and linear movements: full-step, half-step, and micro-step drive modes. For driving the linear stepper motor, the micro-step drive mode was used.

The mathematical equations for the implemented stepper motor, which is a hybrid stepper motor, are differential equations for the dynamic model of the stepper motor, including the electrical equations, and the mechanical equations of the implemented hybrid stepper motor [34].

$$\frac{dia}{dt} = \frac{va+km.\omega.\sin(N.\theta)-Ria}{L} \tag{Eq.1}$$

$$\frac{dib}{dt} = \frac{vb+Km.\omega.\cos(N.\theta)-Ria}{L} \tag{Eq.2}$$

$$\frac{d\omega}{dt} = \frac{Km.ib.\cos(N.\theta)-T-Km.ia.\sin(N.\theta)-Kv.\omega}{J} \tag{Eq.3}$$

$$\frac{d\theta}{dt} = \omega \tag{Eq.4}$$

Where, (Eq.1) and (Eq.2) are electrical equations, and (Eq.3) and (Eq.4) are the mechanical equations for the modeled system. In these equations, the parameters of phase A include  $va$  (the voltage) and  $ia$  (the current) of phase A of the stepper motor. Similarly, the parameters of phase B include  $vb$  (the voltage) and  $ib$  (the current) of phase B of the stepper motor. Also,  $\omega$  is the rotor rotational speed (rad/s),  $T$  is the load torque (N.m), and  $\theta$  is the rotor angular position (rad).

The control system has been modeled in MATLAB/SIMULINK software by using the designed control system and stepper motor's characteristics. Fig. 5 illustrates the designed model of the control system for controlling the hybrid stepper motor. The designed model includes a signal generator, current subsystem, position subsystem, voltage supply, and three scopes for monitoring the generated waveforms.



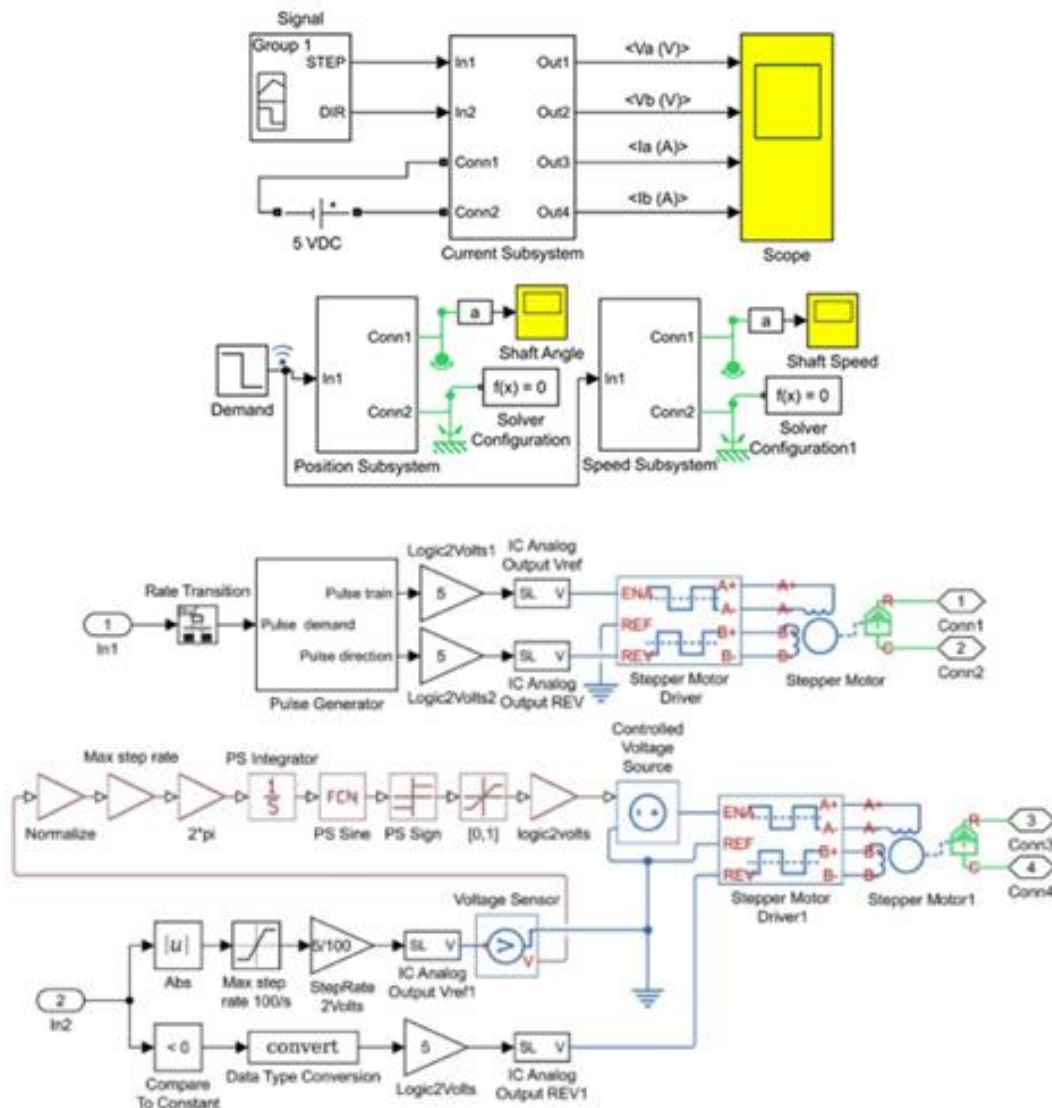
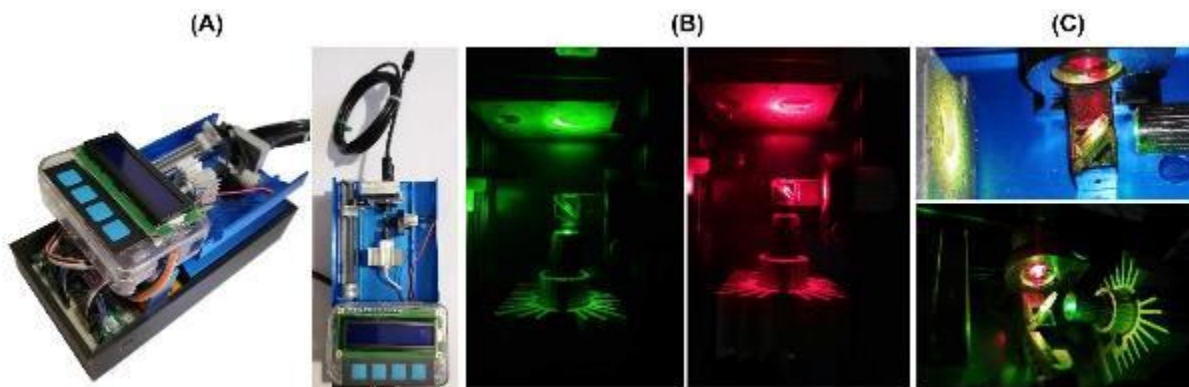


Fig. 5. The overall simulation model.

**2.3. Development of the Device and the Experimental Setup**

After the design and the modeling of the system, the prototype of the LLLT device was developed. Fig. 6 (A) illustrates the prototyped device. The control system is connected to the motor driver unit as well as the laser driver unit and it can control the performance of these units. By transmitting the control commands and driving sequences of the stepper motor’s phases, the control unit can control the performance and the activation of the linear stepper motor. By using this method, controlling the positioning of the focus lens with a high resolution is possible. Meanwhile, the

control unit can control the activation sequences of the laser modules as well as their output power. The optical prism, which is placed in front of the laser modules, can align the laser lights. The optical prism directs the emitted laser lights onto the entrance of the optical fiber which is precisely fixed in front of the emitted laser light. Therefore, the generated laser light, with controlled intensity and frequency, can be transferred to the desired healing zone through the optical cable. Fig. 6 (B) illustrates the device running in the single-wavelength green (532 nm) and red (650 nm) LLLT modes, and Fig. 6 (C) shows the device working in the multi-wavelength mode.



**Fig. 6.** (A) The prototyped device, (B) The laser beams run in single-wavelength mode (C) The laser beams run in multi-wavelength mode.

An experimental study was performed to validate the performance of the control system and to evaluate the functionality of the developed device in generating low-level laser lights with desired working factors. In the first phase of the experiment, the functionality of the control system in controlling the linear position of the focus lens was evaluated. In this phase, the stepper motor was driven with predetermined working factors to evaluate the accuracy and the repeatability of the linear movement. The stepper motor was driven while varying the rotor speed, as presented in Table 1, and the accuracy of the system in executing the desired travel length was measured. A digital caliper, 0–300 mm with a precision of 0.01 mm and a resolution of 0.01 mm, was used to measure the travel length of the carriage.

**Table 1.** The details of the positioning test.

Test number	Repeat cycle	Rotational speed (rpm)	Travel length (mm)
T1	5	10	10
T2	5	30	10
T3	5	60	10
T4	5	10	5
T5	5	30	5
T6	5	60	5
T7	5	10	2
T8	5	30	2
T9	5	60	2

In the second phase of the experiment, the carriage of the stepper motor was interacted with a digital force sensor to measure the executed pushing force. In this phase of the experiment, the stepper motor was operated with a rotational speed of 10 rpm while the carriage of the stepper motor was pushing the force sensor in an interaction with the solid fixtures. In the third phase of the experiment, the functionality of the

control system in driving the laser modules and controlling the intensity of the generated laser lights, were evaluated. The conditions of the laser emission test are presented in Table 2.

**Table 2.** The laser emission test conditions.

Test group TR	Red laser	
	Condition	intensity
TR1	Continuous	100%
TR2		80%
TR3		50%
TR4		20%
TR5		10%
Test group TG	Green laser	
	Condition	intensity
TG1	Continuous	100%
TG2		80%
TG3		50%
TG4		20%
TG5		10%
Test group TM	Multi-Wavelength laser light	
	Condition	intensity
TM1	Continuous	100%
TM2		80%
TM3		50%
TM4		20%
TM5		10%

### 3. RESULTS AND DISCUSSION

The simulation of the designed model was executed in MATLAB/SIMULINK software. In the designed system, micro-step mode was used for driving the linear stepper motor. After setting the working parameters as well as the specifications of the stepper

motor and the controller, the simulation was run for 0.1 sec. Fig. 7 presents the simulation results.

In Fig. 7 (A) and (B),  $V_a$  illustrates the voltage of phase A and  $V_b$  illustrates the voltage of phase B in the stepper motor.  $I_a$  shows the current in phase A and  $I_b$  shows the current in phase B of the stepper motor. It can be seen in the generated voltage and current waveforms that both voltage and current waveforms have a  $90^\circ$  displacement between phase A and phase B. Also, the electrical current waveforms are similar to sine and cosine waveforms. This shows that the control

system has the functionality to generate proper signals for driving the stepper motor. Fig. 7 (C) and (D) presents the generated waveforms for the shaft angle and the shaft speed of the stepper motor. It can be seen in the generated waveforms that the control system can precisely control the positioning of the motor's shaft while smoothly driving the linear system. It can be seen that the shaft speed changes according to the micro-step driving mode. The simulation results show that the designed control system, as well as the driving technique, works well in different driving conditions.

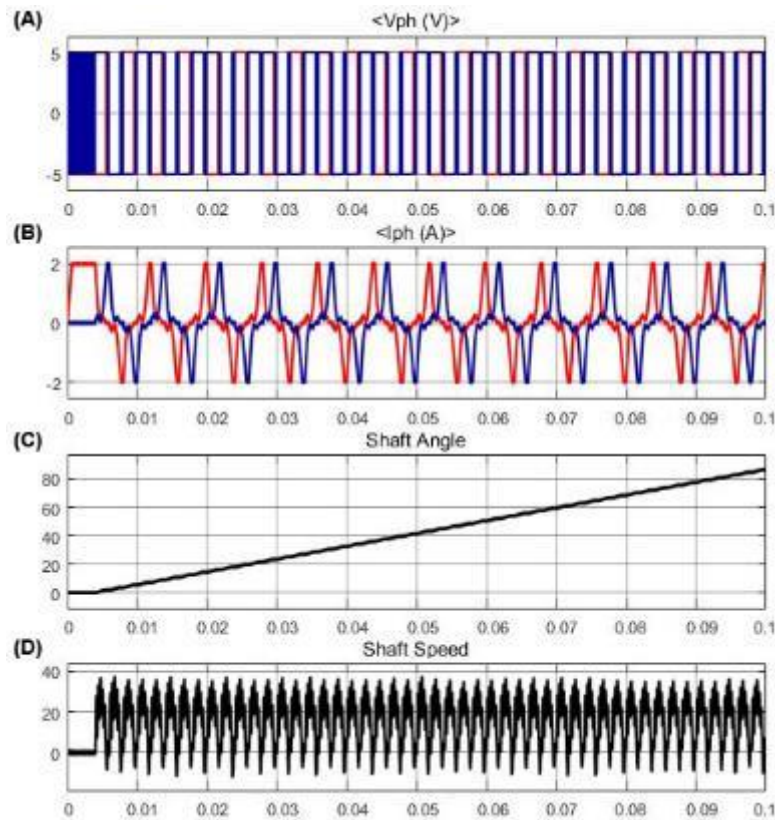


**Fig. 7.** The simulation results: (A) voltage, (B) current, (C) shaft angle, and (D) shaft speed waveforms of the modeled stepper motor.

After the modeling of the control system, experimental tests were conducted to evaluate the functionality of the control system in driving the linear stepper motor for positioning the focus lens. In the experimental study, the stepper motor was operated using the designed control system while varying the shaft speed and the length of the carriage travel. In each test, the executed travel was measured so that the error accrued in the execution of the movement as well as the

positioning accuracy of the focus lens can be calculated. According to the theory and calculated values, the focus lens position can be set in a linear axis with a position accuracy of 0.78 micrometers. However, in practice, there are different factors negatively affecting the positioning accuracy of the linear stepper motor. The details of this phase of the experimental verification are presented in Table 3 and Table 4.

**Table 3.** The test conditions and the measured position of the stepper motor's carriage.

Test number	Travel length (mm)	Rotational speed (rpm)	Repeat cycle	Measured travel length (mm)					
				Test #1	Test #2	Test #3	Test #4	Test #5	



T1	10	10	5	10.03	10.01	10.02	9.99	10.02
T2	10	30	5	10.04	10.05	10.01	10.04	10.05
T3	10	60	5	10.05	10.04	10.02	10.03	10.04
T4	5	10	5	5.01	5.01	5.02	5.00	5.01
T5	5	30	5	5.02	5.03	5.02	5.03	5.02
T6	5	60	5	5.03	5.01	5.05	5.03	5.04
T7	2	10	5	2.01	2.02	1.99	2.01	2.01
T8	2	30	5	2.00	2.01	2.01	2.00	2.02
T9	2	60	5	2.04	2.02	2.03	2.03	2.04

**Table 4.** The test conditions and the obtained results of the positioning accuracy.

Test number	Repeat cycle	Rotational speed (rpm)	Travel length (mm)	Average measured Travel (mm)	Average travel error (mm)	Maximum travel error ( $\mu\text{m}$ )
T1	5	10	10	10.014	0.014	30
T2	5	30	10	10.038	0.038	50
T3	5	60	10	10.036	0.036	50
T4	5	10	5	5.01	0.01	20
T5	5	30	5	5.024	0.024	30
T6	5	60	5	5.032	0.032	50
T7	5	10	2	2.008	0.008	20
T8	5	30	2	2.008	0.008	20
T9	5	60	2	2.032	0.032	40

It can be seen that the higher the rotational speed used, the lower the positioning accuracies became. Therefore, the results of the positioning accuracy reveal that lower rotational speeds for rotating the shaft of the stepper motor can provide a better accuracy in the positioning of the linear stepper motor's carriage. It can be seen from the results, as well as in the generated graph, that the rotational speed of the 10 (rpm) in a distance of 10 mm has an average linear positioning error of 14 microns, the rotational speed of the 10 (rpm) in a distance of 5 mm has an average linear positioning error of 10 microns, and the rotational speed of the 10 (rpm) in a distance of 2 mm has an average linear positioning error of 8 microns. It can be deduced from the results that better results, in terms of the positioning accuracy of the stepper motor's carriage, can be obtained when the stepper motor is driven with a rotational speed of 10 rpm. Thus, the rotational speed of 10 rpm has been used in the configuration of the stepper motor driver for driving the stepper motor.

In the second phase of the experiment, the carriage of the stepper motor interacted with a digital force sensor to measure the generated pushing force. The structure was fixed to the ground using super glue. The digital force meter and the device were fixed using solid fixtures. The generated pushing force was measured while the stepper motor was operated with a rotational speed of 10 rpm. The stepper motor was

capable of generating 0.54 N pushing force during the experiment. Therefore, the carriage of the stepper motor can move the focus lens, which is fixed to the carriage, with a sufficient pushing/pulling force.
















In the third phase of the experiment, the capability of the developed system and the method of generating red and green laser lights were evaluated. In this phase of the experiment, different intensities were used for generating the laser light. Also, different activation sequences, including continuous and intermittent emission approaches, were considered in this phase of the experiment. Table 5 presents the conditions of the performed test.

It can be seen that the developed system, can generate laser lights with predetermined working factors. It can be seen from the results that, in all testing conditions, the control system can generate laser lights in single- and multi-wavelength laser emission modes. It can be seen that the laser module can generate continuous and intermittent laser light emissions, with the desired intensity. The working parameters of the LLLT device, including the intensity and the activation sequences of the laser lights can be set using an HMI unit. The device can be run in single- or multi-wavelength modes. Therefore, different ranges of the laser light wavelengths as well as different intensities of the laser light can be used during a reconstruction process. In addition, by using an optical fiber cable, the generated laser light can be transferred

onto the distraction zone, which can be suited inside the body. Therefore, the designed system can be used as

both intro-oral and extra-oral solutions for assisting the DO process.

**Table 5.** Conditions of the laser light emission test.

Test	Test conditions								
	Laser wavelength	Condition	Intensity	Output/Results	Laser wavelength	Condition	Intensity	Output/Results	
Single-Wavelength mode				Multi-wavelength mode					
TR 1	650 nm	Continuous	100%		TM 1	650 nm and 532 nm	Continuous	100%	
TR 2	650 nm	Continuous	80%		TM 2	650 nm and 532 nm	Continuous	80%	
TR 3	650 nm	Continuous	50%		TM 3	650 nm and 532 nm	Continuous	50%	
TR 4	650 nm	Continuous	20%		TM 4	650 nm and 532 nm	Continuous	20%	
TR 5	650 nm	Continuous	10%		TM 5	650 nm and 532 nm	Continuous	10%	
TG 1	532 nm	Continuous	100%						
TG 2	532 nm	Continuous	80%						
TG 3	532 nm	Continuous	50%						
TG 4	532 nm	Continuous	20%						
TG 5	532 nm	Continuous	10%						

**4. CONCLUSIONS AND FUTURE WORK**

PSTs, including photonic, mechanical, electrical, and electromagnetic techniques, have recently been developed to be used during the DO process. These methods can improve the conditions of the treatment and shorten the treatment time. LLLT is a category of photonic stimulation techniques that have shown

positive effects when used during the DO treatment. In this work, a novel LLLT solution has been designed and developed to be used during DO treatment in MRA. The developed device can generate laser lights with specific wavelengths and transfer them onto the distraction zone. The proposed LLLT device can be used in single- and multi-wavelength modes during the

DO treatment, with controlled output power of the laser light and the activation intervals. The device can generate the desired LLLT to be used during the DO treatment.

The DO technique is a novel solution for the reconstruction of congenital and acquired defects in the maxillofacial area. PSTs have recently been developed to assist the DO process and to improve the quality of the outcome of the treatment. Recently, novel systems, including LLLT devices, have been developed for assisting the DO process. However, these developments have been limited to the design and verification of the systems and their functionality. In the future, research needs to be done on the application of these devices in animal studies and human trials.

## REFERENCES

- [1] Goldwaser, B.R., et al., "Automated continuous mandibular distraction osteogenesis: review of the literature". *Journal of Oral and Maxillofacial Surgery*, Vol. **70**(2), pp. 407-416, 2012.
- [2] Hatefi, S., et al., "Review of automatic continuous distraction osteogenesis devices for mandibular reconstruction applications". *BioMedical Engineering OnLine*, Vol. **19**(1), pp. 1-21, 2020.
- [3] Peacock, Z.S., et al., "Bilateral Continuous Automated Distraction Osteogenesis: Proof of Principle". *The Journal of craniofacial surgery*, . Vol. **6**(8), pp. 2320-2324, 2015.
- [4] Li, Y., et al., "Overview of methods for enhancing bone regeneration in distraction osteogenesis: potential roles of biometals". *Journal of orthopaedic translation*, Vol. **27**, pp. 110-118, 2021.
- [5] Singh, M., et al., "Biological basis of distraction osteogenesis—a review". *Journal of Oral and Maxillofacial Surgery, Medicine, and Pathology*, Vol. **28**(1), pp. 1-7, 2016.
- [6] Mofid, M.M., et al., "Callus stimulation in distraction osteogenesis". *Plastic and reconstructive surgery*, Vol. **109**(5), pp. 1621-1628, 2002.
- [7] Mofid, M.M., et al., "Craniofacial distraction osteogenesis: a review of 3278 cases". *Plastic and reconstructive surgery*, Vol. **108**(5), pp. 1103-14; discussion 1115-7, 2001.
- [8] Swennen, G., R. Dempf, and H. Schliephake, "Cranio-facial distraction osteogenesis: a review of the literature. Part II: experimental studies". *International Journal of Oral and Maxillofacial Surgery*, Vol. **31**(2), pp. 123-135, 2002.
- [9] Dasukil, S., et al., "Unpredicted bilateral device breakage during active phase of mandibular distraction: A case report and literature review". *Journal of Stomatology, Oral and Maxillofacial Surgery*, 2020.
- [10] Fu, R., et al., "Mechanical regulation of bone regeneration during distraction osteogenesis". *Medicine in Novel Technology and Devices*, Vol. **11**, pp. 100077, 2021.
- [11] Hatefi, S., et al., "Review of physical stimulation techniques for assisting distraction osteogenesis in maxillofacial reconstruction applications". *Medical Engineering & Physics*, Vol. **91**, pp. 28-38, 2021.
- [12] Yılmaz, B.T., et al., "In vivo efficacy of low-level laser therapy on bone regeneration". *Lasers in Medical Science*, pp. 1-8, 2022.
- [13] Cakarar, S., et al., "Acceleration of consolidation period by thrombin peptide 508 in tibial distraction osteogenesis in rats". *British Journal of Oral and Maxillofacial Surgery*, Vol. **48**(8), pp. 633-636, 2010.
- [14] Miloro, M., J.J. Miller, and J.A. Stoner, "Low-level laser effect on mandibular distraction osteogenesis". *Journal of oral and maxillofacial surgery*, Vol. **65**(2), pp. 168-176, 2007.
- [15] Karu, T., "Photobiology of low-power laser effects". *Health phys*, Vol. **56**(5), pp. 691-704, 1989.
- [16] Gurler, G. and B. Gursoy, "Investigation of effects of low level laser therapy in distraction osteogenesis". *Journal of stomatology, oral and maxillofacial surgery*, Vol. **119**(6), pp. 469-476, 2018.
- [17] Landucci, A., et al., "Efficacy of a single dose of low-level laser therapy in reducing pain, swelling, and trismus following third molar extraction surgery". *International journal of oral and maxillofacial surgery*, Vol. **45**(3), pp. 392-398, 2016.
- [18] Hatefi, K., et al., "Design of Laser-Assisted Automatic Continuous Distraction Osteogenesis Device for Oral and Maxillofacial Reconstruction Applications". *Majlesi Journal of Electrical Engineering*, Vol. **13**(4), pp. 135-145, 2019.
- [19] Liu, X., et al., "Effect of lower-level laser therapy on rabbit tibial fracture". *Photomedicine and laser surgery*, Vol. **25**(6), pp. 487-494, 2007.
- [20] Massotti, F.P., et al., "Histomorphometric assessment of the influence of low-level laser therapy on peri-implant tissue healing in the rabbit mandible". *Photomedicine and laser surgery*, Vol. **33**(3), pp. 123-128, 2015.
- [21] Garcia, V.G., et al., "Effect of LLLT on autogenous bone grafts in the repair of critical size defects in the calvaria of immunosuppressed rats". *Journal of Cranio-Maxillofacial Surgery*, Vol. **42**(7), pp. 1196-1202, 2014.
- [22] Aragão-Neto, A.C., et al., "Combined therapy using low level laser and chitosan-policaju hydrogel for wound healing". *International journal of biological macromolecules*, Vol. **95**, pp. 268-272, 2017.
- [23] de Oliveira Gonçalves, J.B., et al., "Effects of low-level laser therapy on autogenous bone graft stabilized with a new heterologous fibrin sealant". *Journal of Photochemistry and*

- Photobiology B: Biology*, Vol. **162**, pp. 663-668, 2016.
- [24] Bosco, A.F., et al., "Effects of low-level laser therapy on bone healing of critical-size defects treated with bovine bone graft". *Journal of Photochemistry and Photobiology B: Biology*, Vol. **163**: p. 303-310, 2016.
- [25] Hübler, R., et al., "Effects of low-level laser therapy on bone formed after distraction osteogenesis". *Lasers in medical science*, Vol. **25**(2): p. 213-219, 2010.
- [26] Freddo, A.L., et al., "Effect of low-level laser therapy after implantation of poly-L-lactic/polyglycolic acid in the femurs of rats". *Lasers in medical science*, Vol. **24**(5), pp. 721-728, 2009.
- [27] Cerqueira, A., et al., "Bone tissue microscopic findings related to the use of diode laser (830nm) in ovine mandible submitted to distraction osteogenesis". *Acta cirurgica brasileira*, Vol. **22**(2), pp. 92-97, 2007.
- [28] Freddo, A.-L., et al., "A preliminary study of hardness and modulus of elasticity in sheep mandibles submitted to distraction osteogenesis and low-level laser therapy". *Medicina oral, patologia oral y cirugia bucal*, Vol. **17**(1), pp. e102, 2012.
- [29] Abd-Elaal, A., et al., "Evaluation of the effect of low-level diode laser therapy applied during the bone consolidation period following mandibular distraction osteogenesis in the human". *International journal of oral and maxillofacial surgery*, Vol. **44**(8), pp. 989-997, 2015.
- [30] Freddo, A.L., et al., "Influence of a magnetic field and laser therapy on the quality of mandibular bone during distraction osteogenesis in rabbits". *Journal of Oral and Maxillofacial Surgery*, Vol. **74**(11): p. 2287. e1-2287. e8, 2016.
- [31] Taha, S.K., et al., "Effect of Laser Bio-Stimulation on Mandibular Distraction Osteogenesis: An Experimental Study". *Journal of Oral and Maxillofacial Surgery*, Vol. **76**(11), pp. 2411-2421, 2018.
- [32] Abdelaal, A.Z. and F.A. Saad, "Estimation of the therapeutic effect of diode laser on bone cells in mandibular distraction osteogenesis: An experimental study in adult male rabbits". *Egyptian Journal of Histology*, Vol. **44**(4), pp. 902-915, 2021.
- [33] Center, H.M. *Photonic Stimulation*. Available from: <https://www.healthmedicinecenter.net/photonic-stimulation.htm>.
- [34] Baluta, G. and M. Coteata. "Precision microstepping system for bipolar stepper motor control. in *Electrical Machines and Power Electronics, 2007*". *ACEMP'07. International Aegean Conference on*. 2007. IEEE.